

8-1-1985

Magnetoresistance Method To Determine GaAs and Alxga1-Xas Mobilities in Alxga1-Xas/GaAs Modulation-Doped Field-Effect Transistor Structures

David C. Look

Wright State University - Main Campus, david.look@wright.edu

George B. Norris

W. Kopp

T. Henderson

H. Morkoç

Follow this and additional works at: <https://corescholar.libraries.wright.edu/physics>



Part of the [Physics Commons](#)

Repository Citation

Look, D. C., Norris, G. B., Kopp, W., Henderson, T., & Morkoç, H. (1985). Magnetoresistance Method To Determine GaAs and Alxga1-Xas Mobilities in Alxga1-Xas/GaAs Modulation-Doped Field-Effect Transistor Structures. *Applied Physics Letters*, 47 (3), 267-269.
<https://corescholar.libraries.wright.edu/physics/30>

This Article is brought to you for free and open access by the Physics at CORE Scholar. It has been accepted for inclusion in Physics Faculty Publications by an authorized administrator of CORE Scholar. For more information, please contact library-corescholar@wright.edu.

Magnetoresistance method to determine GaAs and $\text{Al}_x\text{Ga}_{1-x}\text{As}$ mobilities in $\text{Al}_x\text{Ga}_{1-x}\text{As}/\text{GaAs}$ modulation-doped field-effect transistor structures

D. C. Look and George B. Norris

University Research Center, Wright State University, Dayton, Ohio 45435

W. Kopp, T. Henderson, and H. Morkoç

Department of Electrical Engineering and Coordinated Science Laboratory, University of Illinois, Urbana, Illinois 61801

(Received 5 March 1985; accepted for publication 13 May 1985)

Charge carrier mobilities are conveniently measured in simple, *homos*tructure field-effect transistors (FET's) by means of the geometric magnetoresistance (GMR) technique.

*Hetero*structure FET's, however, are more complicated because of multiple conducting regions, as well as multiple conducting bands within a given region. We apply a multilayer GMR mobility model to a frequently used heterostructure FET design, namely, the $\text{Al}_{0.3}\text{Ga}_{0.7}\text{As}/\text{GaAs}$ modulation-doped FET (MODFET). By analyzing the results at different magnetic fields, we can separate the contributions of the various GaAs subbands and the $\text{Al}_{0.3}\text{Ga}_{0.7}\text{As}$ conduction band. In the particular MODFET structure studied here, the lowest GaAs subband mobility ranges from $5.7 \times 10^3 \text{ cm}^2/\text{Vs}$ at threshold to $6.9 \times 10^3 \text{ cm}^2/\text{Vs}$ at saturation, while the $\text{Al}_{0.3}\text{Ga}_{0.7}\text{As}$ mobility is about $5 \times 10^2 \text{ cm}^2/\text{Vs}$. This is the first time that the various mobilities in MODFET structures have been separately measured.

Perhaps two of the most important parameters affecting the operation of an electronic device are the charge carrier concentration and the mobility. It is, of course, desirable to measure these quantities on the device itself rather than on a special test structure. One important device, the field-effect transistor (FET), is ideally suited for making mobility measurements by the geometric magnetoresistance (GMR) technique, because the FET geometry shorts out the Hall electric field which would normally exist in the presence of a perpendicular magnetic field.¹ Furthermore, carrier concentration can be determined on the same device by measurements of gate capacitance versus gate voltage. In recent years, the GMR technique has been applied by several groups to study mobility profiles in GaAs MESFET's (metal-semiconductor FET's).²⁻⁷ Note that the GaAs MESFET is a relatively simple system because only one conductive material is involved, and it is straightforward, with some exceptions, to determine both carrier concentration and depletion depth from capacitance data. Thus, accurate mobility and carrier concentration depth profiles may be obtained.

In a heterostructure, however, the picture is much more complicated. Consider, e.g., the $\text{Al}_x\text{Ga}_{1-x}\text{As}/\text{GaAs}$ MODFET (modulation-doped FET), which has already proven to be a very fast switching device as well as a high-frequency amplifier.⁸ Here, electron conduction can take place in three regions: (1) the $\text{Al}_x\text{Ga}_{1-x}\text{As}$; (2) the GaAs near the heterointerface, at which conduction subbands are formed; (3) the GaAs buffer layer and substrate. The interpretation of capacitance is also no longer simple, and a numerical approach is necessary.^{9,10} The object of this paper is to apply a generalized GMR analysis to heterostructures. The new model allows the separate determination of the $\text{Al}_x\text{Ga}_{1-x}\text{As}$ and GaAs mobilities by measuring a higher order (than B^2) magnetic field dependence of the resistance. This procedure also requires a separation of the capacitance contributions of the two regions. We apply the mobility and capacitance analyses to a MODFET structure grown by molecular beam epitaxy.

We define the *measured* average and differential GMR mobilities, respectively, in the usual manner:

$$\mu_A^2 = \frac{1}{B^2} \left(\frac{G_0}{G_B} - 1 \right), \quad (1)$$

$$\mu_D^2 = \frac{1}{B^2} \left(\frac{(dG/dV_G)_0}{(dG/dV_G)_B} - 1 \right), \quad (2)$$

where $G (\equiv I_{SD}/V_{SD})$ is the conductance, B is the magnetic field strength, and the subscript zero denotes $B = 0$. Here V_G is the Schottky-barrier gate voltage, which establishes a depletion region. In a *homos*tructure MESFET, the depletion depth is given by $d = \epsilon A/C$, where ϵ is the dielectric constant, A the gate area, and C the gate capacitance. Then μ_D , in Eq. (2), may be simply interpreted⁷ as the mobility at depth d , i.e., $\mu_D = \mu(d)$.

In a MODFET structure the situation is more complicated, and we must use a multilayer GMR analysis. The measured quantities, μ_A^2 and μ_D^2 , must now be interpreted differently, as follows¹¹:

$$\mu_A^2 = \frac{\sum n_i \mu_i^3}{1 + \mu_i^2 B^2} \bigg/ \sum \frac{n_i \mu_i}{1 + \mu_i^2 B^2}, \quad (3)$$

$$\mu_D^2 = \frac{\sum \frac{C_i \mu_i^3}{1 + \mu_i^2 B^2} \left(1 + \frac{n_i}{\mu_i} \frac{d\mu_i}{dn_i} \frac{3 + \mu_i^2 B^2}{1 + \mu_i^2 B^2} \right)}{\sum \frac{C_i \mu_i}{1 + \mu_i^2 B^2} \left(1 + \frac{n_i}{\mu_i} \frac{d\mu_i}{dn_i} \frac{1 - \mu_i^2 B^2}{1 + \mu_i^2 B^2} \right)}, \quad (4)$$

where n_i and C_i denote, respectively, the *sheet* carrier concentration and capacitance of the i th group of electrons, with mobility μ_i . Here i can denote $\text{Al}_x\text{Ga}_{1-x}\text{As}$ electrons, substrate electrons, or electrons in one of the heterointerface subbands. (If μ_i for a given electron group varies with depth in a given region, then the sum should be approximated by an integral within this region.) In Eq. (4) we have approximated $d\mu_i/dV_G \simeq (d\mu_i/dn_i) (dn_i/dV_G) \propto C_i (d\mu_i/dn_i)$. Later, we

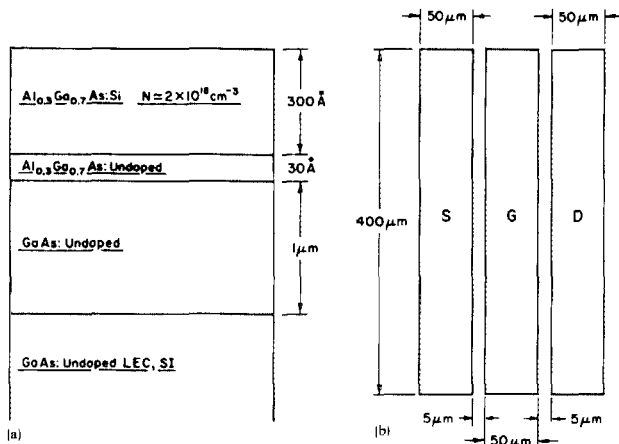


FIG. 1. (a) Cross-sectional view of the MBE heterostructure used in this experiment. The dimensions are not drawn to scale. (b) Fat FET geometry used for the C - V and GMR measurements.

will simply allow this term to be a fitting parameter. If one group of electrons, say group j , is totally dominant, then $\mu_A \approx \mu_j$, at any magnetic field, and μ_D is only weakly field dependent. In general, however, μ_A and μ_D will depend upon B , and this dependence can then be used to separately determine the various μ_i . In the data presented here, $\mu_D > \mu_A$, but this inequality does not always hold.

As seen from Eqs. (3) and (4), it is first necessary to fit the capacitance data, and determine the C_i and n_i for each electron group. A detailed discussion of this determination is the subject of a separate paper.¹⁰ Note that the weighting factor, in the numerator, is μ_i^3 , which strongly favors the high-mobility regions. It should also be mentioned that Eqs. (3) and (4) are derived in the relaxation-time approximation, and for an energy-independent relaxation time. It is easy to allow for an energy-dependent relaxation time and to then carry along a "scattering factor" in the calculations. However, in forward bias, at least, the electrons are nearly degenerate in the lowest subband, and the scattering factor would then be close to unity anyway. Even in reverse bias, the energy-independence approximation probably does not appreciably affect the results. The relaxation-time approximation itself, however, is more serious since it is known not to hold for polar optical-mode scattering, an important mechanism in GaAs at room temperature. Even so, the magnetic field dependences will probably be close to those given here, as is the case in the single-layer problem.

The model was tested on a typical MBE layered structure which was designed for FET applications. The various layer thicknesses and dopings are given in Fig. 1(a). The capacitance and GMR mobility were both measured on the same "fat FET" test structure [Fig. 1(b)], with a $50 \times 400 \mu\text{m}$ gate. (Note that small gate-length FET designs also work well for the GMR measurements.) The experimental capacitance was then fitted with a first-principles theory,¹⁰ and the results are shown in Fig. 2. It should be noted that the lowest subband capacitance C_0 increasingly dominates the other subband capacitances as V_G is increased (positively), but that the $\text{Al}_x\text{Ga}_{1-x}\text{As}$ capacitance, C_{AlG} , takes over at about 0.5 V forward bias. The sheet carrier concentration (not shown) of the $\text{Al}_x\text{Ga}_{1-x}\text{As}$, however, never becomes as large as that of the lowest subband. Therefore, we would expect to see the

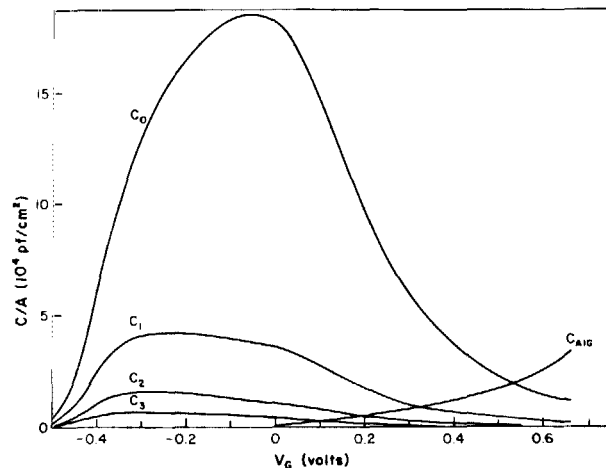


FIG. 2. Various capacitance contributions, as determined from a theoretical fit of the C - V data. The GaAs subbands, beginning at the lowest, are represented by C_0 , C_1 , C_2 , C_3 , respectively, and the free electrons in the $\text{Al}_x\text{Ga}_{1-x}\text{As}$ are represented by C_{AlG} .

effects of μ_{AlG} in μ_D , but not in μ_A .

The mobility results are presented in Fig. 3. The solid lines are theoretical fits to Eqs. (3) and (4), solved simultaneously. The fitted parameters are the following: μ_0 , the lowest subband mobility; μ_1 , representing the next three subbands above the lowest; μ_{AlG} , the $\text{Al}_x\text{Ga}_{1-x}\text{As}$ mobility; and $D \equiv d\mu_i/dn_i$, assumed equal for all subbands, and zero for the $\text{Al}_x\text{Ga}_{1-x}\text{As}$. (The fitted parameter D actually should be larger than $d\mu_i/dn_i$, since it really includes *all* contributions to $d\mu_i/dV_G$. Indeed, our results will verify this fact, since we can calculate $d\mu_0/dn_0$ after the fitting. Also, we could introduce a separate D_i for each subband, but the present data do not justify this complication.) It is clear that the data can be fitted very well with the μ_0 vs V_G curve shown in Fig. 3, and an $\text{Al}_{0.3}\text{Ga}_{0.7}\text{As}$ mobility of $5 \times 10^2 \text{ cm}^2/\text{Vs}$. This μ_{AlG} is a very reasonable value for the given doping concentration.¹² For the present sample, it could be varied about 20% without giving unreasonably poor fits. The μ_0 , on the other hand, could not be varied more than 1–2% without appreciably degrading the fit. Thus, this method gives excellent values for the most important mobility parameter in the system, namely, μ_0 .

Unfortunately, the other subband mobilities are harder

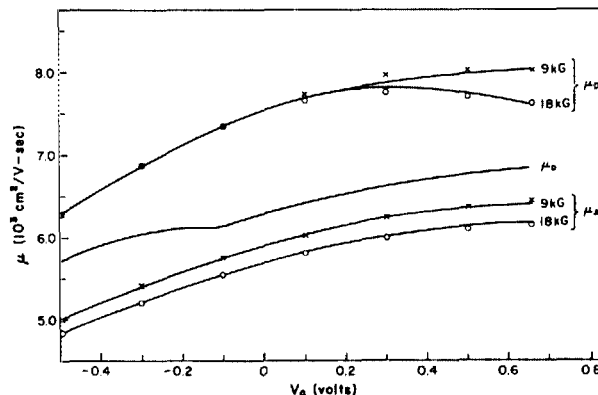


FIG. 3. Average (μ_A) and differential (μ_D) experimental mobilities, each at 9 kG (\times) and 18 kG (\circ). The solid lines through the points are theoretical fits of Eqs. (3) and (4). The line designated μ_0 is the lowest subband mobility, a fitted parameter.

to determine accurately, since these upper subbands affect the overall conductivity and capacitance much less than the lowest subband. Our combined mobility parameter μ_1 varies from about $2.2 \times 10^3 \text{ cm}^2/\text{Vs}$ at high forward bias to about $3.0 \times 10^3 \text{ cm}^2/\text{Vs}$ at high reverse bias near threshold. According to a well-known theory of two-dimensional scattering¹³ the upper subbands should have lower mobilities than the lowest subband, as confirmed in the data. However, a detailed theory, including all the important scattering mechanisms at room temperature, does not exist yet, so a comparison is difficult. It should also be mentioned that the μ_1 , and especially the μ_{AIG} fitted values, in the forward-bias region, depend upon the $\text{Al}_x\text{Ga}_{1-x}\text{As}$ free-electron capacitance, which in turn depends upon the donor activation energy E_D in the $\text{Al}_x\text{Ga}_{1-x}\text{As}$.^{12,14} For our capacitance fit we assumed $E_D = 66 \text{ meV}$.¹² However, μ_0 is nearly unaffected by the choice of E_D .

The fitted values of the parameter D are typically about a factor two higher than the subsequently computed values of $d\mu_0/dn_0$ for this sample. This is a quite reasonable agreement in view of our previous discussion of D , as well as the fact that a mere 1–2% change in μ_0 at a given point would bring the slope at that point into agreement with D . Thus, all of our fitted parameters, μ_0 , μ_1 , μ_{AIG} , and D , are well within the expected values, and confirm the general validity and usefulness of the model. Note from Fig. 3 that Eqs. (1) and (2), if interpreted in the usual way, would have given a quite misleading interpretation for the calculated mobility because of the multiband effects. Similar considerations hold for the more commonly used Hall-effect measurements. Thus, multilayer systems must be carefully analyzed, especially when $\mu B \gtrsim 1$. On the other hand, the resulting magnetic field dependences allow much more information to be gleaned from the analysis.

Finally, it should be stated that a fit of μ_A [Eq. (3)] alone is sufficient to give good values of μ_0 and μ_1 . This fact is important, because a μ_A measurement [Eq. (1)] gives much better S/N than the corresponding μ_D measurement [Eq. (2)]. However, to determine μ_{AIG} , it is absolutely necessary to measure μ_D , at least for this sample and probably for most similar samples.

We would like to thank T. A. Cooper for the electrical measurements, D. E. Johnson for drawing the figures, and J. Montanaro for typing the manuscript. The work of DCL and GBN was performed at the Avionics Laboratory, Wright-Patterson AFB, Dayton, Ohio, under USAF contract F33615-84-C-1423.

- ¹J. R. Sites and H. H. Wieder, IEEE Trans. Electron Devices ED-27, 2277 (1980).
- ²P. R. Jay and R. H. Wallis, IEEE Electron. Devices Lett. EDL-2, 265 (1981).
- ³W. Ford and J. Barrera, in *Semi-Insulating III-V Materials*, Evian, edited by S. Makram-Ebeid and B. Tuck (Shiva, Nantwich, 1982), p. 352.
- ⁴R. H. Wallis and P. R. Jay, in *Semi-Insulating III-V Materials*, Evian, edited by S. Makram-Ebeid and B. Tuck (Shiva, Nantwich, 1982), p. 344.
- ⁵D. J. Sheldon, R. J. Higgins, R. H. Wallis, and R. Koyama, Bull. Am. Phys. Soc. 28, 490 (1983).
- ⁶D. C. Look, S. Chaudhuri, A. Ezis, and M. Moloney, in *Semi-Insulating III-V Materials*, Kah-nee-ta, 1984, edited by D. C. Look and J. S. Blake-more (Shiva, Nantwich, 1984), p. 397.
- ⁷D. C. Look, J. Appl. Phys. 57, 377 (1985).
- ⁸T. P. Pearsall, Surf. Sci. 142, 529 (1984).
- ⁹B. Vinter, Appl. Phys. Lett. 44, 307 (1984).
- ¹⁰George B. Norris, D. C. Look, W. Kopp, J. Klem, and H. Morkoç, J. Vac. Sci. Technol. B 3, 797 (1985); Appl. Phys. Lett. 47, 15 Aug (1985).
- ¹¹D. C. Look (unpublished).
- ¹²N. Chand, T. Henderson, J. Klem, W. T. Masselink, R. Fischer, Y.-C. Chang, and H. Morkoç, Phys. Rev. B 30, 4481 (1984).
- ¹³S. Mori and T. Ando, J. Phys. Soc. Jpn. 48, 865 (1980).
- ¹⁴E. F. Schubert and K. Ploog, Phys. Rev. B 30, 7021 (1984).

Improvements in the modulation amplitude of submicron gratings produced in *n*-InP by direct photoelectrochemical etching

R. M. Lum, F. W. Ostermayer, Jr.,^{a)} P. A. Kohl,^{a)} A. M. Glass,^{a)} and A. A. Ballman
AT&T Bell Laboratories, Holmdel, New Jersey 07733

(Received 25 March 1985; accepted for publication 14 May 1985)

The modulation amplitude of gratings produced by maskless etching techniques decreases rapidly at spatial frequencies $> 500 \text{ mm}^{-1}$. This has limited the usefulness of these techniques for producing the submicron gratings required for distributed feedback lasers. We report improvements as large as a factor of 100 in the direct photoelectrochemical (PEC) etching of gratings in *n*-InP which were accomplished by changing the composition and concentration of the electrolyte solutions. Measurements on the PEC etching characteristics of *n*-InP in HF, HCl, HBr, and H_2SO_4 solvents are presented.

Direct holographic recording of submicron gratings in III-V materials by liquid phase photoetching has been demonstrated using both photochemical (PC)¹⁻⁴ and photoelec-

trochemical (PEC)⁵ techniques. Maskless techniques for producing gratings have potential application in the fabrication of distributed feedback (DFB) lasers which are currently made by a multistep photoresist process.^{6,7} However, gratings produced by PC⁴ and PEC⁵ etching exhibit an abrupt

^{a)} AT&T Bell Laboratories, Murray Hill, NJ 07974.